Np(V) complexation with propionate in 0.5–4 M NaCl solutions at 20–85 °C

Aleksandr N Vasiliev, Nidhu L Banik, Remi Marsac, Daniel R Froehlich, Jörg Rothe, Stepan Kalmykov, Christian M. Marquardt

▶ **To cite this version:**

Aleksandr N Vasiliev, Nidhu L Banik, Remi Marsac, Daniel R Froehlich, Jörg Rothe, et al.. Np(V) complexation with propionate in 0.5–4 M NaCl solutions at 20–85 °C. Dalton Transactions, 2015, 44 (8), pp.3837 - 3844. 10.1039/C4DT03688C . hal-01904329

HAL Id: hal-01904329
https://hal.science/hal-01904329

Submitted on 7 Jan 2019

HAL is a multi-disciplinary open access archive for the deposit and dissemination of scientific research documents, whether they are published or not. The documents may come from teaching and research institutions in France or abroad, or from public or private research centers.

L'archive ouverte pluridisciplinaire **HAL**, est destinée au dépôt et à la diffusion de documents scientifiques de niveau recherche, publiés ou non, émanant des établissements d'enseignement et de recherche français ou étrangers, des laboratoires publics ou privés.

Np(V) complexation with propionate in 0.5 – 4 M NaCl solutions at 20-85°C†

Aleksandr N. Vasiliev[1,3], Nidhu L. Banik*[,1], Rémi Marsac[1], Daniel R. Froehlich[1,2], Jörg Rothe[1], Stepan. N. Kalmykov[3], Christian M. Marquardt[1]

Low molecular weight organics (LMWO; e.g. acetate, propionate, lactate) can significantly impact the speciation and mobility of radionuclides in aqueous media. Natural clay rock formations, considered as a potential host rock for nuclear waste disposal, can contain significant amount of organic matter. There is few thermodynamic data reported for the complexation of pentavalent actinides with LMWO, especially at elevated temperature conditions, relevant for assessing the long-term safety of disposal options for heat-producing high-level nuclear waste. In the present study, the complexation of Np(V) with propionate is studied by spectroscopic techniques in 0.5 – 4 M NaCl solutions under systematic variation of ligand concentration and temperature. Slope analysis shows the formation of the 1:1 NpO_2-propionate complex (NpO_2Prop). The local structure of the NpO_2-propionate complex is determined by Extended X-ray Absorption Fine Structure spectroscopy and suggests that propionate binds to Np(V) in a bidentate mode. Using the specific ion interaction theory (SIT), the stability constant at zero ionic strength and 25°C is determined as log $\beta^\circ_{1,1} = 1.26 \pm 0.03$. The stability constants increase continuously with increasing temperature between 20–85 °C. The log β_0 values are linearly correlated to the reciprocal temperature, indicating $\Delta_r H^0_m$ = const. and $\Delta_r C^0_{p,m} = 0$, allowing the calculation of $\Delta_r H^0_m$ and $\Delta_r S^0_m$ for the formation of the NpO_2-propionate complex from the integrated van't Hoff equation. The thermodynamic evaluations indicate that the reaction is endothermic and entropy driven.

Introduction

Neptunium (Np) is an actinide element located between uranium and plutonium in the periodic table of the elements. The environmental chemistry of this radioactive alpha-emitting element is of considerable interest due to the long half-life of its main isotope ^{237}Np ($t_{1/2} = 2\times10^6$ a) and its high solubility and potentially high mobility as pentavalent NpO_2^+ forming under non-reducing conditions. It is known that Np can exist in oxidation states between +III and +VII in aqueous systems, with tetra- and pentavalent Np (Np(IV), (V)) being clearly the most stable and relevant oxidation states in the geosphere[1].

The long-term disposal of high-level nuclear waste materials will be performed in deep geological formations. For this purpose, different host rocks such as clay[2,3] or crystalline formations[2-5] are investigated. Detailed predictions of the geochemical behavior of key radionuclides including Np is necessary for the long-term safety assessment of a potential disposal site and concept. A reliable understanding and thermodynamic description of chemical processes affecting the aqueous chemistry of Np in the tetra- and pentavalent oxidation states is therefore a topic of key interest. Radionuclide sorption to the host rock material is known as an efficient retention factor, immobilising radionuclides in case of release from the waste. Dissolved natural organic compounds are ubiquitous in the environment. Like inorganic ligands commonly found in the environment (e.g. CO_3^{2-}, OH^-), they can bind to metals and potentially increase the radionuclide mobility by forming dissolved complexes with sometimes significantly less tendency towards sorption. Previous characterization of dissolved organic compounds (DOC) in the pore waters of the Callovo-Oxfordian (COx) and Opalinus Clay (OPA) formations show that low molecular weight organic compounds (LMWO) represent a large fraction of the whole DOC (COx: 88 %, OPA: 36 %). Acetate and propionate play an important role with concentrations up to 1865 and 127 µM, respectively[6,7]. Larger organic molecules such as humic substances are also found at some potential nuclear waste disposal sites[8]. Their composition and structure is highly complex, but it was shown that, by using thermodynamic complexation data for LMWO which can be considered as main "building blocks" of humics, their complexation properties for a given cation/radionuclide combination can be predicted with reasonable precision[9,10]. Hence, thermodynamic data derived for LMWO like propionate is relevant in a broader scientific and applied context.

Due to the radioactive decay heat of high active waste, increased temperatures up to about 100 °C are expected in the near-field of a repository[11] in clay rock formation. It was previously shown that apparent complex formation constants between radionuclides and LMWO tend to increase with temperature[12]. Various groundwater compositions are observed depending on the disposal site considered. For instance, OPA exhibits pore waters with ionic strengths between I = 0.3-0.5 M (e.g. reported in[7]). In contrast to this, markedly saline conditions are found in ground water characteristic of clay formations in northern Germany (I > 3.5 M)[13]. Thus it becomes necessary assess the effect of ionic strength and temperature on Np(V) complexation with LMWO to predict its potential mobilisation from a nuclear waste repository under specific scenarios. Although the interaction of Np(V) with LMWO is particularly relevant in this context, only few studies aimed at determining the corresponding complex formation constants. The proprionate ligand was also not included in the data evaluation performed within the NEA-TDB project on actinide-organics complexation Hummel et al 2005.[14]

In the present study, the complexation of Np(V) with

propionate is studied by spectrophotometry as a function of NaCl concentration, ligand concentration, and temperature. The local structure of the dominant Np(V)-propionate complex is determined by Extended X-ray Absorption Fine Structure (EXAFS) spectroscopy. Ionic strength effects are treated with the specific ion interaction theory (SIT)[15]. Using this approach, the temperature dependent thermodynamic stability constants and $\Delta_r H^0_m$ and $\Delta_r S^0_m$ of the complexation reaction are determined.

Materials and Methods

Chemicals and Np(V) stock solution

All chemicals were of p.a. quality or better and obtained from Merck (Darmstadt, Germany) or Riedel de Haen (Seelze, Germany). All experiments were conducted using de-ionized "MilliQ" water (ρ = 18.2 MΩ cm^{-1}). A radiochemically well characterized ^{237}Np(V) stock solution (5 mM) in 0.01 M HCl was used for all complexation experiments. ^{237}Np concentration was determined by liquid scintillation counting (LSC) with α/β descrimination of the ^{233}Pa daughter nuclide, using the scintillation cocktail Ultima Gold XR (Packard Instruments Co., USA) and the liquid scintillation counter (LSC) Tri-Carb (Packard Instruments Co., USA).

Sample preparation

All concentrations given in mol L^{-1} (molarity, M) were corrected to mol kg^{-1} H_2O (molality, m) for later calculations to avoid changes in the concentration due to changes in solution density by temperature and ionic strength. The concentration of Np(V) was held at 2×10^{-5}-6×10^{-5} M for UV-Vis/NIR experiments. Samples were usually equilibrated for 1-2 days prior to measurement. Complexation of Np(V) with propionate in NaCl solution was studied by two independent series of measurements. A first set of samples was prepared at different NaCl concentrations (I = 0.5–4.0 M) with total propionate concentration ($[Prop]_{tot}$) being varied from 0.03 to 0.1 M to determined the ionic strength dependence of Np(V)-propionate complexation at room temperature. The ionic strength was adjusted with solid NaCl and pHc was adjusted to 5 with aliquots of 0.01 M HCl. A second set of samples was prepared at constant I = 0.5 M, $[Prop]_{tot}$ varying from 0.03 and 0.1 M and T varying from 20 to 85°C using a constant temperature circulator (Thermo Haake DL30-W45/B Open-Bath, Germany) to determined the temperature dependence of Np(V)-propionate complexation. pHc was adusted to 5 at room temperature, before raising T. In addition, two series of samples at various $[Prop]_{tot}$ for I = 0.5 M and T = 23 and 85°C were prepared at pHc = 7 to confirm the results obtained for pHc =5.

For EXAFS measurements, the samples were prepared at 4 different [NaCl] (from 0.5 to 4.37 m) at constant propionate concentrations of 0.48 M and constant Np(V) concentration of 0.77 mmol·L^{-1} (pHc = 5.5-5.1; Table S1).

pH measurements

In the present study, measurements of operational pH values were performed with an Orion 2 Star Benchtop pH meter using an Orion 8103SC combination pH electrode. Commercial pH Titrisol buffer concentrates (Merck p.a.) were used to calibrate the setup at room temperature. For pH measurements at I > 0.1 m, an empirical correction term was applied for the measured operational pH-values (pH_{exp}) to obtain thermodynamically well-defined quantities. An empirical correction coefficient (A) that depends on background electrolyte composition and concentration and that has been accurately determined in our laboratories for aqueous NaCl systems and at room temperature[16] was used to correct the operational pH_{exp} values according to equations 1 and 2:

$$pH_C = pH_{exp} + A_{NaCl} \quad (1)$$

$$A_{NaCl} = 0.0013 * (m_{NaCl})^2 + 0.1715 * m_{NaCl} - 0.0988 \quad (2)$$

where m_{NaCl} is the molality of the background electrolyte. The pHc is a measurement of the molality of the proton (-log $[H^+]$) and is only made here at room temperature. Knowing the apparent proton dissociation constant of propionate for a given ionic strength at room temperature (K_a), as described further below, the total concentration of proton in the sample can be calculated ($[H^+]_{tot} = [H^+] + [HProp]_{eq}$, where HProp is the protonated form of propionate). Because $[H^+]_{tot}$ does not vary with T, it is used for the calculation of the free propionate concentration ($[Prop^-]_{eq}$) for highet T, where pHc is not measured.

Calculation of free propionate concentration

Note that all concentrations are calculated as molality in the following sections. Proton dissociation of the propionic acid must be taken into account as only the free propionate ($Prop^-$) will interact with NpO_2^+. The free propionate concentration as a function of I and T is determined as follows:

$$[Prop^-]_{eq}(\mathrm{I},\mathrm{T}) = \frac{-\left([H^+]_{tot} - [Prop]_{tot} + K_a\ (T)\right)}{2} + \frac{\sqrt{\left([H^+]_{tot} - [Prop]_{tot} + K_a\ (T)\right)^2 - 4[Prop]_{tot}K_a\ (T)}}{2} \quad (3)$$

The apparent proton dissociation constant (K_a) depends on the ionic strength and the temperature:

$$K_{a,0}(T) = K_a(T) \times \frac{\gamma(H^+)(T)\times\gamma(Prop^-)(T)}{\gamma(HProp)(T)} \quad (4)$$

where $K_{a,0}$ refers to the thermodynamic constant at zero ionic strength. Its variation with temperature can be found in literature[17]. Activity coefficients (γ) are calculated according to the specific ion interaction theory (SIT) recommended by the NEA-TDB[18]. The SIT can be applied to ionic strengths up to 3.2 m to deduce the complex formation constant at I = 0. Activity coefficients for an aqueous species "i" with a charge Z are calculated as follows:

$$\log \gamma_i = -Z^2 \frac{A(T)\sqrt{I}}{1+1.5\sqrt{I}} + \sum_k \varepsilon(i,k) \times m_k$$

$$= -Z^2 D + \sum_k \varepsilon(i,k) \times m_k \qquad (5)$$

where D is the Debye-Hückel term used in SIT, m_k is the molality of the aqueous species k, ε(i,k) is the specific ion interaction coefficient between species i and k. The variation of ε(i,k) with temperature in the presently studied temperature range can be neglected, thus the 25°C values are used for all ionic strength corrections. ε(H^+,Cl^-) is known and ε(Na^+,$Prop^-$) is estimated by analogy with acetate (both values given in [23]). A(T) is the limiting Debye-Hückel law slope, which depends on temperature:

$$A(T) = e^3 \sqrt{\frac{2\pi N\rho}{1000(k\epsilon T)^3}} \qquad (6)$$

where N is the Avogadro number, e stands for absolute electronic charge, ϵ is here the dielectric constant of water at the given temperature, ρ is the pure water density, k is the Boltzman constant, and T is absolute temperature (Kelvin). Using, eq. 3-6, $[H^+]_{tot}$ is firstly determined as a function of pHc and $[Prop]_{tot}$ at room temperature, which is required for the calculations of $[Prop^-]_{eq}$ for other T.

UV-Vis analysis and data treatment

UV-VIS/NIR spectroscopy measurements were carried out at constant pHc= 5 and 7 with Np(V) concentration of 2×10^{-5}-6×10^{-5} M in 1 cm quartz cuvettes using a Varian Cary-5 spectrophotometer. The spectroscopic absorption range was analysed from 950 nm to 1030 nm. A constant temperature circulator (Haake, Germany) was used to keep the samples at the required fixed temperature while taking the absorption spectra. The concentrations of NpO_2^+ in solution were determined by peak deconvolution of the UV-Vis/NIR spectra. The deconvolution was performed assuming the absorption peak area as being the sum of two Gaussian functions for the Neptunyl cation and the Np-propionate complex. The unknow peak maximum of the complex was constrained the same for all the samples within one series of spectra recorded for constant I and T and varying $[Prop]_{tot}$. The uncertainty on Np(V) speciation determination was estimated to be 5% with the present approach.

XAFS spectroscopy.

All four EXAFS samples were prepared under argon atmosphere. The EXAFS samples were transferred into a vial mounted inside an Ar-flushed cell which acts as second containment, at the same time keeping sample vials inside an anoxic atmosphere.[19] EXAFS measurements were performed at the 2.5 GeV synchrotron light source ANKA (KIT, Germany) at the INE-Beamline for Actinide Research.The INE-Beamline is equipped with a double-crystal monochromator (Si(111), Si(311), InSb(111), and Ge(422) crystal pairs) and a mirror focussing system (Rh coated silicon mirrors). X-ray absorption spectra were collected in fluorescence mode using the 5 pixel high purity germanium solid state detector (Canberra Ultra-LEGe). The detector was positioned at an angle of 90° relative to the incoming beam. A detailed description of the design of the INE-Beamline can be found elsewhere.[19,20] For energy calibration a Zr foil was measured simultaneously with each sample. The data evaluation was performed using the software packages Athena 0.8.061[21] and EXAFSPAK.[22] In all cases the ionization energy (E_0) was set to 17610 eV. Theoretical scattering phases and amplitudes were calculated with FEFF8.40[23] using the crystal structure of $NH(C_2H_5)_3[UO_2(CH_3COO)_3]$[24] and replacing U by Np. The best theoretical model was fit to the k^2-weighted raw Np L_{III}-edge EXAFS data using the Marquardt algorithm included in EXAFSPAK. The amplitude reduction factor S_0^2 was set to 0.9.

Results and discussion

Experimental UV-Vis/NIR results

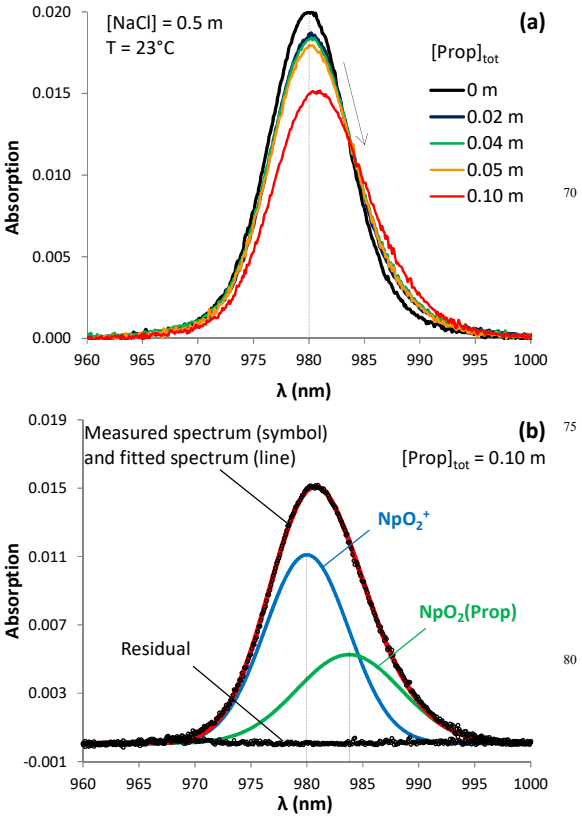

Fig. 1(a) Np(V) absorption spectra for various propionate concentrations (0-0.3M) at $[Np(V)]_{tot} = 5.94\times10^{-5}$ M, I = 0.51 m; T = 23°C. b) Example of a deconvoluted spectrum ([Prop] = 0.1 m; I = 0.51 m; pHc = 5.0, T = 23°C.

Fig.1(a) – the absorption spectra of Np(V) in presence of propionatein [NaCl] = 0.51 m for T = 23°C and pHc = 5 – exemplarily shows the spectrophotometric results of Np(V)-propionate complex formation in [NaCl] solution and T = 23°C. Generally, as the concentration of propionate increases, the intensity of the absorption band of free NpO_2^+ at 980 nm decreases and the maximum of the absorption band is shifting to higher wavelength. This is an indication that the NpO_2^+ ion

is complexed by forming a new absorption band at higher wavelengths caused by the Np(V)-propionate complex. Peak deconvolution of the spectra allows the determination of a single complex, as exemplified in Fig. 1(b) for one spectrum. According to the peak deconvolution performed within the present study, the absorption band of the Np(V)-propionate complex has its maximum at ~984 nm, similar to the 1:1 Np(V)-acetate complex[25]. Spectral changes with increasing propionate concentration while keeping I and T constants are similar for all temperatures as illustrated in Fig. S1 for I = 0.5 m and T = 85°C, or in Fig. S2 for I = 3.2 m and T = 23°C. Spectral changes are also similar to those observed in a previous study[26], in which $NpO_2(Prop)\cdot nH_2O$ compounds (n = 1, 2) were synthesized for $[Prop]_{tot}$ = 0.2 M at pH = 6.5. NpO_2^+-Cl^- complexation has no significant effect on the spectra, as shown by Neck et al.[27] at room temperature up to I =1.0-3.0 m. Since the experiments up to T = 85°C were presently made for I = 0.5 m, NpO_2^+-Cl^- complexation is very likely negligible at higher T.

Effect of ligand concentration

The complexation reaction of one NpO_2^+ion with "n" propionate ligands (denoted by $Prop^-$) can be described as:

$$NpO_2^+ + n\ Prop^- \leftrightarrow NpO_2(Prop)_n^{(1-n)} \quad (7)$$

The conditional stability constant (β, in kg mol^{-1}) is:

$$\beta = \frac{[NpO_2(Prop)_n^{(1-n)}]}{[NpO_2^+][Prop^-]_{eq}^n} \quad (8)$$

The concentrations ratio of the Np(V) species is determined by peak deconvolution of the UV-vis spectra. Note that the amount of $NpO_2(Prop)_n^{(1-n)}$ is negligible compared to $[Prop^-]_{eq}$ under chosen experimental conditions, and do not appear in the expression of $[Prop^-]_{eq}$ (eq. 3). Slope analysis allows the determination of log β and the stoichiometry of the reaction:

$$\log\frac{[NpO_2(Prop)_n^{(1-n)}]}{[NpO_2^+]} = \log\beta + n\times\log[Prop^-]_{eq} \quad (9)$$

The experimental data are plotted in Fig. 2 according to eq. 9 for three different titration series. Results for T = 23°C are compared to T = 85°C (both in [NaCl] = 0.51 m solution), to show the effect of temperature on the complexation reaction. Comparison to the plot at T = 23°C and [NaCl] = 3.20 m demonstrates the effect of ionic strength. The slopes (n = 1.05 ± 0.05 at 23°C; 0.99 ± 0.11 at 85°C; 1.04 ± 0.15 for I = 3.2 m) confirm the formation of an 1:1 NpO_2^+-propionate complex.

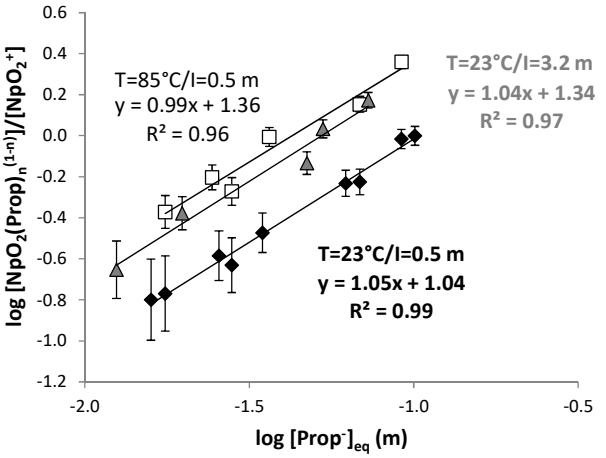

Fig. 2 Slope analysis of the Np(V)-propionate complex formed at 23 and 85°C for [NaCl] = 0.51m, and 23°C for [NaCl] = 3.2 m. Slopes ≈ 1 (1.05±0.05 and 0.99±0.11 for both T, respectively, 1.04 ± 0.15 for I = 3.2 m) indicate the formation of the 1:1 complex. Log β (conditional) increases both with temperature and ionic strength (from 1.04±0.06 to 1.36±0.13).

The y-intercept, log β, is determined as 1.04 ± 0.06 at 23°C and increases with temperature (1.36 ± 0.13 at 85°C) and with ionic strength (1.34 ± 0.15 at 3.2 m). The same stoichiometry is found at ionic strengths from 0.51 to 3.2 m or T from 20 to 85 °C. During the data analysis, it appeared that only the 1:1 complex was observable both for pHc = 5 and 7 within the range of $[Prop]_{tot}$ investigated. Therefore, data for pHc = 5 and 7 were treated together (i.e. two series for pHc = 7 with I = 0.51 m, T = 23 and 85°C).

Effect of ionic strength

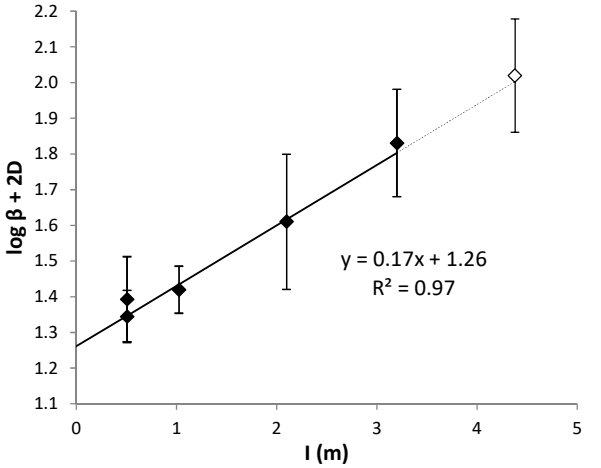

Fig. 3 SIT plot of the equilibrium reaction $NpO_2^+ + Prop^- \rightleftharpoons NpO_2(Prop)$ in NaCl, yielding $\log\beta_0 = 1.23 \pm 0.03$. The white symbol ([NaCl] = 4.2 m) shows data outside the recommended applicability of the SIT (data not used in the regression). The dotted line shows the extrapolation of the results obtained for lower I to 4.2 m.

By systematically varying the background electrolyte concentration, in this case the NaCl concentration, at constant T and applying an appropriate model for activity coefficients (γ) it

is possible to extrapolate the conditional equilibrium constants β to zero ionic strength (β_0) standard conditions.

$$\beta_0 = \beta \times \frac{\gamma(NpO_2(Prop))}{\gamma(NpO_2^+)\times\gamma(Prop^-)} \quad (10)$$

The combination of eq. 5 and eq. 10 gives:

$$\log\beta - \Delta Z^2 \times D = \log\beta_0 - \Delta\varepsilon \times I \quad (11)$$

where $\Delta Z^2 = \Sigma\ Z^2(\text{products}) - \Sigma\ Z^2(\text{aducts}) = -2$ for the reaction given in eq. 7, involving one propionate in the complex, and $\Delta\varepsilon = \varepsilon(Na^+ + Cl^-; NpO_2(Prop)) - \varepsilon(Na^+; Prop^-) - \varepsilon(Cl^-; NpO_2^+)$. Experimental data are plotted according to eq. 11 in Fig. 3, where log β+2D evolves linearly with I, as expected. From the slope, Δε is obtained as -0.17 ± 0.03 and the y-intercept (log β_0) equals to 1.26 ± 0.03. Log β_0 and Δε are in agreement with previously determined values for NpO_2-actetate complexation at 25°C[25]. Using $\varepsilon(Cl^-; NpO_2^+) = 0.09 \pm 0.05$ and assuming $\varepsilon(Na^+; Prop^-) = 0.08 \pm 0.01$ by analogy with acetate, $\varepsilon(Na^+ + Cl^-; NpO_2(Prop))$ would not be significantly different from to zero, which is expected for a non-charged species in accordance with SIT. Note that we have investigated Np(V)-propionate complexation up to 4.2 m, which is outside the recommened validity range of SIT. Therefore, this data are not used for the regression as indicated by the dotted lines in Fig. 3. However, in this case it is obvious that the SIT approach remains applicable even above its usually accepted applicability limit.

Effect of temperature

Temperature effect on the NpO_2^+ complexation by propionate was investigated between 20 and 85°C, for [NaCl] = 0.51 m at pHc = 5 and 7. Log β(T) are corrected to I = 0 for each temperature by applying the SIT as described in the previous section to obtain log β_0(T) (Table S1). As a first approach, heat capacity was hypothesized to be zero as observed, for instance, in a recent Cm(III)-propionate complexation study[28], i.e. the molal standard reaction enthalpy $\Delta_rH^0_m$ and entropy $\Delta_rS^0_m$ do not vary with temperature between 20 and 85°C. Following this simplification, $\Delta_rH^0_m$ and $\Delta_rS^0_m$ can be obtained from an Arrhenius plot on the basis of the van't Hoff equation

$$\log\beta_0(T) = -\frac{\Delta_rH^0_m}{RTln(10)} + \frac{\Delta_rS^0_m}{Rln(10)} \quad (12)$$

where R is the ideal gas constant. Fig. 4 shows the plot of log β_0(T) versus 1/T. The NpO_2(Prop) complex formation reaction significantly increases over about half an order of magnitude when increasing temperature from 20°C to 80°C. A linear relationship is observed, confirming the initial hypothesis of zero heat capacity. $\Delta_rH^0_m$ and $\Delta_rS^0_m$ are calculated as 10.9 ± 1.2 kJ mol^{-1} and 62 ± 4 J mol^{-1} K^{-1}, respectively. Both values are positive, showing that the formation of the NpO_2(Prop) complex is endothermic and entropy driven. Positive $\Delta_rH^0_m$ and $\Delta_rS^0_m$ are likely due to dehydration effects of NpO_2^+ and $Prop^-$ ions.

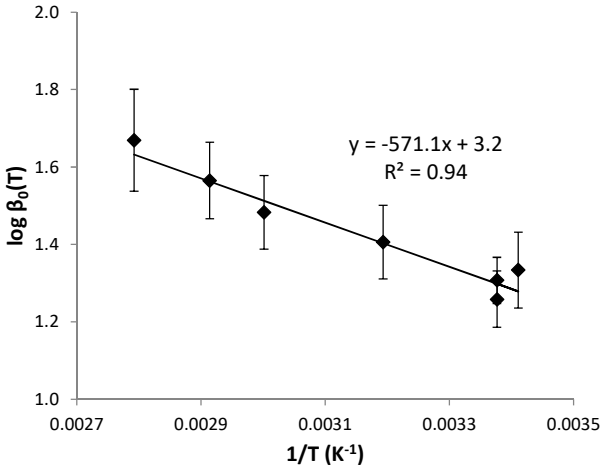

Fig. 4 Np(V)-propionate complexation constant extrapolated to zero ionic strength (log β_0) versus the reciprocal of the temperature (K^{-1}).

Comparison of thermodynamic data with literature data

The thermodynamic parameters of the complex formation reaction between Np(V) and propionate obtained in this study are summarized in Table 1.

Table 1. Thermoydynamic data and model parametersfor Np(V)-propionate complex formation in NaCl solution determined in the present study. Uncertainties are reported at ± 1σ confidence level. Individual ε(i,k) values are estimated based on $\varepsilon(Na^+; Acetate^-)$ value.

Parameter	$NpO_2^+ + Prop^- \rightleftharpoons NpO_2(Prop)$
log β_0(25°C)	1.26 ± 0.03
Δε (in NaCl)	-0.17 ± 0.03
$\varepsilon(NpO_2^+; Cl^-)$[23]	0.09 ± 0.05
$\varepsilon(Na^+; Prop^-)$[23]	0.08 ± 0.01
$\varepsilon(Na^+ + Cl^-; NpO_2Prop)$	0.00 ± 0.06
$\Delta_rH^0_m$ (kJ M^{-1})	10.9 ± 1.2
$\Delta_rS^0_m$ (J K^{-1} M^{-1})	62 ± 4

To the authors knowledge, there are no Np-propionate complexation studies at elevated temperature and ionic strength in literature. Data available in literature for highly analog chemical systems were published by Rao et al. (2010) for Np(V) complexation with acetate[25]. They obtained log β_0 and Δε values for the 1:1 NpO_2^+-acetate complex similar to the values for propionate derived in this work, both with NaCl (log β_0 = 1.28 ± 0.04 and Δε = -0.24 ± 0.02) and $NaClO_4$ (log β_0 = 1.27 ± 0.02) used as background electrolyte. At 298.15 K and [$NaClO_4$] = 1.05 m, Rao et al.[25] determined Δ_rH_m = 18.1 ± 1.8 kJ mol^{-1} and Δ_rS_m = 75 ± 6 J mol^{-1} K^{-1}, which are comparable to our present results for the propionate system. In general, positive $\Delta_rH^0_m$ and $\Delta_rS^0_m$ are found for actinide complexes with monocarboxylic ligands, for example, Cm(III)(Prop)$^{+2}$ ($\Delta_rH^0_m$ = 5.7 ± 1.8 kJ mol^{-1} and $\Delta_rS^0_m$ = 84 ± 5 J mol^{-1} K^{-1};[28] or U(VI)(Acetate)$^+$ ($\Delta_rH^0_m$ = 14.5 ± 1.5 kJ mol^{-1} and $\Delta_rS^0_m$ = 104 ± 6 J mol^{-1} K^{-1} [29]. For all these

actinides, the magnitude of $\Delta_r S^0_m$ is comparable because both acetate and propionate coordinate mainly in a bidentate fashion, replacing two water molecules in the first coordination shell of the actinide.

EXAFS

To analyse the structural properties of the Np(V) propionate 1:1 complex as a function of the ionic strength, EXAFS spectroscopy was performed. In the experiments, 0.77 mM Np(V) in the presence of 0.48 M propionate has been investigated at NaCl concentrations of [NaCl] = 0.51, 1.02, 2.09, 4.37 m and at pHc = 5.0-5.5. Details on the composition of the samples are given in Table S2. Spectrophotometric analysis of the samples show that approximately 95 % of the NpO_2(Prop) complex is formed in all EXAFS samples (See Fig. S3). The other ~5% might correspond to the 1:2 or 1:3 complexes, due to the higher $[Prop]_{tot}$ investigated for EXAFS analysis than in the previous sections in this study.

The measured background corrected k^2-weighted Np L_{III}-edge EXAFS spectra are presented together with the related Fourier transforms in Fig. 5. All experimental EXAFS spectra show a comparable pattern. Potential Np-Cl interaction has not been included in the EXAFS fit because room temperature studies on the complexation of Np(V) with chloride showed no contribution of chloride to the EXAFS spectra at $[Cl^-] < 7$ M.[30] The resulting parameters from the EXAFS fit are summarized in Table 2.

Table 2. Structural parameters determined for 0.77 mM Np(V) in the presence of 0.48 M propionate at pH_c = 5.0-5.5 in aqueous NaCl solution ([NaCl] = 0.51, 1.02, 2.09, 4.37 m).
(*held constant during fit, **Np-O_{ax}-Np-O_{ax} multi scattering path is included in the fit, *** σ^2 fixed at 0.003 Å^2).

Structural parameter		Sample in varying NaCl solution (m)			
		0.51	**1.02**	**2.09**	**4.37**
Np-O_{ax}**	N	2*	2*	2*	2*
	R / Å	1.82 (1)	1.82 (1)	1.81 (1)	1.81 (1)
	σ^2 / Å^2	0.002 (1)	0.001 (1)	0.001 (1)	0.001 (1)
Np-O_{eq}	N	4.5 (5)	4.5 (6)	4.7 (7)	4.6 (6)
	R / Å	2.47 (1)	2.47 (1)	2.47 (1)	2.48 (1)
	σ^2 / Å^2	0.007 (2)	0.005 (2)	0.009 (3)	0.007 (2)
Np-C***	N	1.1 (5)	1.0 (5)	0.7 (6)	0.7 (5)
	R / Å	2.88 (4)	2.83 (5)	2.91 (6)	2.87 (7)
ΔE_0 /eV		3.7 (6)	3.7 (6)	3.7 (8)	3.8 (6)
red. error without carbon shell		0.0166	0.0184	0.0226	0.0198
red. error with carbon shell		0.0158	0.0177	0.0224	0.0194
k-range / Å^{-1}		2.85-10.85			

The coordination number of O_{ax} was held constant at 2 in all cases. For all samples a comparable number of about 4.5-4.7 (uncertainty 0.5-0.7) of equatorial oxygen neighbors are found. The axial and equatorial oxygen atoms are located at the distance of 1.81-1.82 and 2.47-2.48 Å, respectively. Due to the low signal-to-noise ratio, the distance of the carbon neighbors shows a higher uncertainty (0.04-0.07 Å) and ranges between 2.83-2.91 Å. However, within the error range these values agree well with structural data reported for acetate complexes of U(VI) (2.87-2.91 Å)[31-34], Np(V) (2.91-2.93 Å)[35], and Np(VI) (2.87 Å)[35]. Accordingly, it can be stated that Np(V)-propionate binding takes place in a bidentate coordination mode as a monodentate binding would lead to a Np-C distance at least 0.3 Å longer, by analogy with Np(VI) (see e.g. Takao et al.[35] and references therein).

Similar binding characteristics were found for U(VI)-acatete complexes[34]. The coordination numbers for carbon (1.1–0.7) agree well with the formation of the 1:1 complex, given the high uncertainty of the coordination number (here determined as ±0.5-0.6 from the fitting procedure).

To proof whether the carbon contribution to the EXAFS oscillation is significant or not, the spectra have either been fitted with or without considering a carbon shell. The reduced errors of both fits are included in Table 2. In all cases, the inclusion of Np-C interaction improves the goodness of the fit indicated by a lower reduced error and, thus, clarifies the presence of propionate in the coordination sphere of Np(V). According to the EXAFS results, showing that propionate binds to NpO_2^+ in a bidentate fashion (Fig. S4), the magnitude of $\Delta_r S^0_m$ value can be attributed to the replacement of two water molecules in the first coordination shell of NpO_2^+ by propionate.

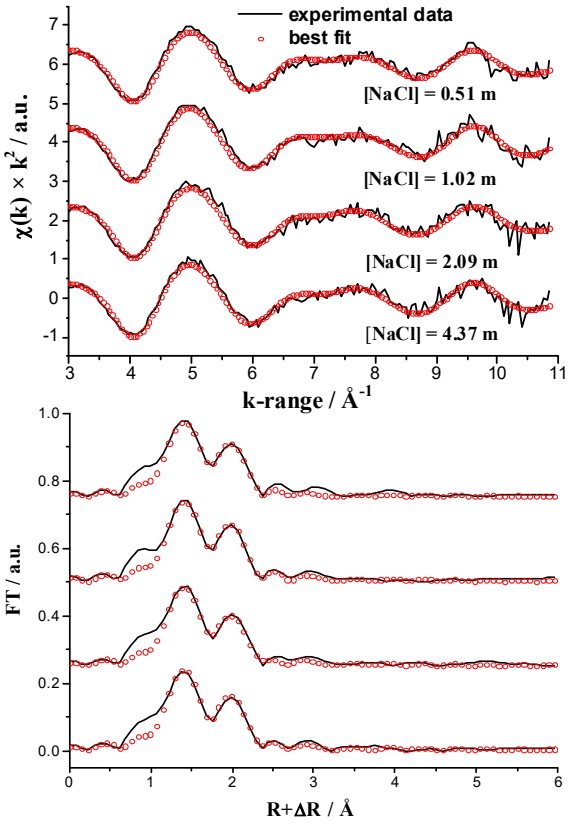

Fig. 5 k^2-weighted Np L_{III}-edge EXAFS spectra (top) and related Fourier transforms (bottom) for 0.77 mM Np(V) in the presence of 0.48 M

propionate at pH_c = 5.0-5.5 in aqueous NaCl solution ([NaCl] = 0.51, 1.02, 2.09, 4.37 m) (fit parameters see Table 2).

Np(V)-propionate complexation at environmentally relevant propionate concentrations

Simulations are made for pHc = 7, with 0.1 and 3 m NaCl and T = 20 and 85°C using the presently obtained Np(V)-propionate complexation parameters in order to test the impact of propionate on Np speciation in more environmentally relevant conditions than the present laboratory study. The percentage of Np(V), in aqueous solutions at pHc 7 present as the NpO_2^+ cation, complexed to propionate versus log $[Prop]_{tot}$ is shown in Fig. 6 ($[Np(V)]_{tot} = 10^{-10}$ m). Although Np(V)-propionate complexation increases with I between 0.1 and 3 m for a given T, or with T between 20 and 85°C for a given I, propionate remains a relatively weak ligand for Np(V) in these conditions: only 1-5 % of Np(V) is bound to propionate for $[Prop]_{tot} = 10^{-3}$ m. In natural clay rocks porewater (e.g. OPA/COx), where propionate is present at lower concentration (127 µM[6,7]) and where Np(V) is in competition with other cations, propionate complexation is expected to have a minor impact on Np(V) speciation.

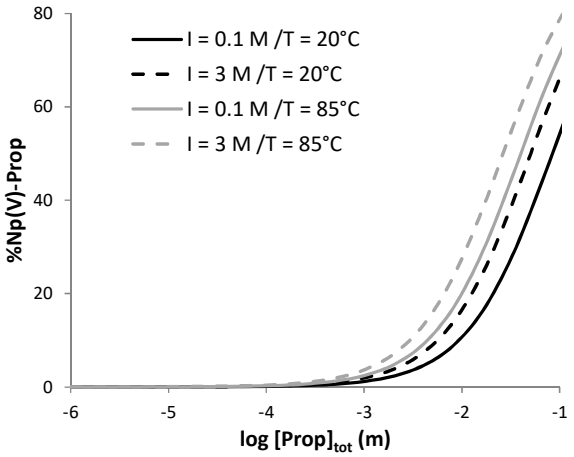

Fig. 6 Calculated percentage of Np(V)-propionate complex ($[Np(V)]_{tot} = 10^{-10}$ m) versus log $[Prop]_{tot}$ for pHc = 7 and I = 0.1 or 3 m and T = 20 or 85°C using thermodynamic parameters determined in this study.

Conclusions

The present study shows that the stability constant for the formation of the 1:1 NpO_2^+-propionate complex, clearly identified as the dominant species under the investigated conditions with log β_0 (25°C) = 1.26 ± 0.03, increases both with ionic strength (0.5 < NaCl < 4.2 m) and temperature (20 < T < 85°C). The complex formation reaction is endothermic and entropy driven, as evidenced by $\Delta_r H^0_m$ = 10.9 ± 1.2 kJ mol^{-1} and $\Delta_r S^0_m$ = 62 ± 4 J mol^{-1} K^{-1}, determined in this work. The magnitude of $\Delta_r S^0_m$ is consistent with a bidentate coordination mode, which is also shown by EXAFS analysis, leading to the replacement of two water molecules in the first coordination shell of NpO_2^+ by the propionate ligand. The newly derived thermodynamic data ($\Delta_r H^0$m, $\Delta_r S^0$m, logβ_0(T)) for Np(V)-propionate complexation are a valuable contribution to thermodynamic databases which are the basis of a reliable safety assessment for nuclear waste disposal scenarios. Using comprehensive modeling tools and the thermodynamic data derived in this work, it becomes possible to predict the potential impact of proprionate (including respective ionic strength and temperature effects) on the geochemical behavior of Np(V). Our predictions indicate that propionate has a minor impact on Np(V) speciation in environmentally relevant propionate concentrations.

Acknowledgment

We would like to thank Mr. T. Hoffmann from the department of radiation protection safety for assistance during sample transport from INE's active laboratories to the INE-Beamline at ANKA. This work has been supported by the German Federal Ministry of Economic Affairs and Energy (BMWi) under Contract No. 02E10206.

Notes and references

* [1]*Karlsruher Institut für Technologie (KIT), Institut für Nukleare Entsorgung, P.O. Box 3640, 76021 Karlsruhe, Germany. Email: nidhu.banik@kit.edu; Tel +4972160822420.*

[2]*Ruprecht-Karls-Universität Heidelberg, Physikalisch Chemisches Institut, Im Neuenheimer Feld 253, 69120 Heidelberg, Germany.*

[3]*Radiochemistry Division, Chemistry Department, Lomonosov Moscow State University, Moscow 119992, Russia.*

†Electronic supplementary information (ESI) available:

1 J. I. Kim, In: Handbook on the Physics and Chemistry of the Actinides. (Freeman, A. J., ed.) Elsevier Science Publishers, B. V., Amsterdam,1986, p. 413.

2 ONDRAF/NIRAS, SAFIR 2: Safety assessment and feasibility interim report, NIROND-2001-06 E, ONDRAF/NIRAS, Brussels/Belgium, 2001.

3 OECD, Safety of geological disposal of high-level and longlived radioactive waste in France – An international peer review of the "Dossier 2005 Argile" concerning disposal in the Callovo-Oxfordian formation, NEA No. 6178, OECD Organization for economic co-operation and development, 2006.

4 P. Hoth, H. Wirth, K. Reinhold, V. Bräuer, P. Krull, H. Feldrappe, Endlagerung radioaktiver Abfälle in tiefen geologischen Formationen Deutschlands – Untersuchung und Bewertung von Tongesteinsformationen, BGR Bundesanstalt für Geowissenschaften und Rohstoffe, Hannover/Germany.

5 H. Geckeis, J. Lützenkirchen, R. Polly, T. Rabung, M. Schmidt,*Chem. Rev.*, 2013, **13,** 1016–1062.

6 A. Courdouan, I. Christl, S. Meylan, P. Wersin, R. Kretzschmar, *Appl. Geochem.,* 2007, **22**, 1537–1548.

7 E. A. Courdouan, I. Christl, S. Meylan, P. Wersin, R. Kretzschmar, *Appl. Geochem*., 2007, **22**, 2926–2939.

[8] F. Claret, T. Schaefer, T. Rabung, M. Wolf, A. Bauer, G. Buckau, *Appl. Geochem.,* 2005, **20**, 1158–1168.

[9] R. F. Carbonaro, D. M. Di Toro, *Geochim. Cosmochim. Acta*, 2007, **71**, 3958–3968.

[10] E. Tipping, S. Lofts, J. Sonke , *Environ. Chem.,* 2011, **8**, 225–235.

[11] J. Brasser, J. Droste, I. Müller-Lyda, J. Neles, M. Sailer, G. Schmidt, M. Steinhoff, Endlagerung wärmeentwickelnder radioaktiver Abfälle in Deutschland, GRS Report, GRS-247, Gesellschaft für Anlagen- und Reaktorsicherheit, 2008.

[12] D. R. Fröhlich, A. Skerencak-Frech, P. J. Panak, *Dalton Trans.,* 2014, **43**, 3958.

[13] D. Bosbach, B. Luckscheiter, B. Brendebach, M. A. Denecke, N. Finck, *J. Nucl. Mater.*, 2009, **385**, 456–460.

[14] W. Hummel, G. Anderegg, I. Puigdomenech, L. Rao, O. Tochiyama, Chemical thermodynamics of compounds and complexes of U, Np, Pu, Am, Tc, Se, Ni and Zr with selected organic ligands, Chemical Thermodynamics Series Volume 9, 2005.

[15] L. Ciavatta, *Annali di Chimica*, 1980, **70**, 551-567.

[16] M. Altmaier, V. Metz, V. Neck, R. Müller, T. Fanghänel, *Geochim. Cosmochim. Acta*, 2003, **67**, 3595-3601.

[17] B. R. McRae, B. A. Patterson, M. L. Origlia-Luster, E. C. Sorenson, E. M. Woolley, *J. Chem. Thermodynamics*, 2003, **35**, 301–329.

[18] R. Guillaumont, T. Fanghänel, J. Fuger, I. Grenthe, V. Neck, D. A. Palmer, M. H. Rand, Chemical thermodynamics Vol. 5. . Update on the chemical thermodynamics of uranium, neptunium. Plutonium, americium and technetium, OECD, NEA-TDB, North Holland, Amsterdam, 2003.

[19] B. Brendebach, N. L. Banik, C. M. Marquardt, J. Rothe, M. A. Denecke, H. Geckeis, *Radiochim.. Acta.,* 2009, **385,** 456-460.

[20] J. Rothe, S. Butorin, K. Dardenne, M.A. Denecke, B. Kienzler, M. Löble, V. Metz, A. Seibert, M. Steppert, T. Vitova, C. Walther, H.Geckeis, *Rev. Sci. Instrum.*, 2012, **83**, 043105/1-13.

[21] B. Ravel, M. J.Newville, *J. Synchrotron Radiat.,* 2005, **12**, 537 - 541.

[22] G.N. George, I. J. Pickering, Stanford/USA, 2000.

[23] A. L Ankudinov, C.E. Bouldin, J.J. Rehr, J. Sims, H. Hung, *Phys. Rev. B,* 2002**, 65***,* 104107/1-11.

[24] L. B. Serezhkina, E.V. Peresypkina, A.V. Virovets, N.A. Neklyudova, *Russ. J. Inorg. Chem.,* 2010, **55**, 1020-1025.

[25] L. Rao, G. Tian, T. G. Srinivasan, P. Zanonato, P. Di Bernardo, *J. Solution Chem,* 2010, **39**,1888–1897.

[26] M. Nakada, T. Yamashita, T. Nakamoto, M. Saeki, N. N. Krot, M. S. Grigor'ev, *Radiochemistry,* 2002, **44**, 97-101.

[27] V. Neck, T. Fanghänel, G. Rudolph, J.I. Kim, *Radiochim. Acta,* 1995, **69**, 39-47.

[28] D. R. Froehlich, A. Skerencak-Frech, M.-L. K. Morkos, P. J. Panak, *New. J. Chem.,* 2013, **37**, 1520.

[29] V. Sladkov, *J. Chem. Thermodynamics,* 2014, **71**, 148–154.

[30] P. G. Allen, J. J. Bucher, D. K. Shuh, N. M. Edelstein, T. Reich, *Inorg. Chem.,* 1997, **36**, 4676-4683.

[31] C. Lucks, A. Rossberg, S. Tsushima, H. Foerstendorf, A. C. Scheinost, G. Bernhard, *Inorg. Chem.*, 2012, **51**, 12288-12300.

[32] J. Jiang, L. Rao, P. Di Bernardo, P. L. Zanonato, A . Bismondo, *J. Chem. Soc., Dalton Trans.*, 2002, **8**, 1832-1838.

[33] E. H. Bailey, J.F.W. Mosselmans, P.F. Schofield, *Geochim. Cosmochim. Acta*, 2004, **68**, 1711-1722.

[34] R. S. Ray, S. Krüger, N. Rösch, *Inorganica Chimica Acta*., 2010, **363**, 263–269.

[35] K. Takao, S. Takao, A. C. Scheinost, G. Bernhard, C. Hennig, *Inorg. Chem.,* 2009, **48**, 8803-8810.